國立臺灣大學理學院物理學系

碩士論文

Department of Physics

College of Science

National Taiwan University

Master's Thesis

利用單 NQ 串標記的量子位元高效編碼來模擬電子組態問題

Using the Qubit-efficient Encoding with the Single NQ-string Labeling to Simulate Electronic Structure Problems

蕭守晏

Shou-Yen Hsiao

指導教授: 管希聖 博士

Advisor: Hsi-Sheng Goan, Ph.D.

中華民國 113 年 7 月

July, 2024

doi:10.6342/NTU202401735

國立臺灣大學碩士學位論文
口試委員會審定書
MASTER'S THESIS ACCEPTANCE CERTIFICATE
NATIONAL TAIWAN UNIVERSITY

利用單 NQ 串標記的量子位元高效編碼來模擬電子組態問題

Using the Qubit-efficient Encoding with the Single NQ-string Labeling to Simulate Electronic Structure Problems

本論文係__蕭守晏__(姓名)_R10222044_（學號）在國立臺灣大學__物理學系__(系/所/學位學程)完成之碩士學位論文，於民國 113 年 7 月 11 日承下列考試委員審查通過及口試及格，特此證明。

The undersigned, appointed by the Department / Institute of _____Physics_____ on _11_(date)_07_ (month)_2024_ (year) have examined a Master's thesis entitled above presented by___Shou-Yen Hsiao___ (name)_____R10222044_____ (student ID) candidate and hereby certify that it is worthy of acceptance.

口試委員 Oral examination committee:

管希聖	張慶瑞	鄭原忠
（指導教授 Advisor）		

doi:10.6342/NTU202401735

摘要

在使用量子處理器模擬電子結構問題時，將量子態對應到量子位元空間的編碼是必要的。在已被提出的編碼方法中，量子位元高效編碼透過僅將正確電子數的量子態編碼到量子位元空間，來減少量子位元的使用量。然而，在使用量子位元高效編碼時，因為對激發算符的直接展開，系統哈密頓量中的包立項數量增長得比其他編碼方法快得多。在量子位元高效編碼的結構下，一種新的標記方法在本論文中被提出，被稱為單 NQ 串標記。使用此標記的目的是通過結合激發算符表達式中的相同項來減少包立項的數量。我們使用單 NQ 串標記的量子位元高效編碼來模擬電子結構問題，並得到了優於使用預設標記的模擬結果。

關鍵字：編碼，量子位元高效編碼，量子變分電路，電子組態問題

doi:10.6342/NTU202401735

doi:10.6342/NTU202401735

Abstract

A fermionic-to-qubit encoding is essential in simulating electronic structure problems with quantum processors. Among the proposed encoding schemes, the qubit-efficient encoding (QEE) reduces the qubit usage to $O(m \log n)$ by only encoding physical configurations to qubit space, compared to other common encoding schemes that need n qubit to simulate the system with n spin-orbitals and m electrons. However, the number of Pauli terms in the QEE Hamiltonian grows much faster than other encoding schemes because of the direct expansion on the excitation operators. Under the structure of QEE, a new labeling method, named single NQ-string labeling, is proposed in this thesis, which aims to reduce the number of Pauli terms by combining similar terms in the expression of excitation operators. Simulations for electronic structure problems using QEE with the single NQ-string labeling are made, and the results outperform those of QEE with default labeling and the parity encoding.

doi:10.6342/NTU202401735

Keywords: Fermionic-to-qubit encoding, Qubit-efficient encoding, Variational quantum eigensolver, Electronic structure problem

doi:10.6342/NTU202401735

Contents

doi:10.6342/NTU202401735

doi:10.6342/NTU202401735

List of Figures

doi:10.6342/NTU202401735

doi:10.6342/NTU202401735

List of Tables

doi:10.6342/NTU202401735

doi:10.6342/NTU202401735

Chapter 1 Introduction

It is believed that quantum computing has the potential to solve some problems that are intractable for classical computers, especially for quantum problems [1]. One of them is the quantum chemistry problem [2], which aims to solve the eigenvalues and eigenfunctions of the time-independent Schrödinger equation. With the superposition and entanglement nature of quantum bits (qubits), several methods have been proposed [3–8] and the runtime for quantum simulations can scale polynomially with the system size [9].

Quantum computing nowadays is still in the Noisy intermediate-scale (NISQ) era [10, 11], which means qubit operations on the processors are reliable in restricted circuit depth, and there is no error correction. The variational quantum eigensolver (VQE) algorithm [12–14] is proposed and can be implemented on NISQ devices. VQE is a hybrid quantum-classical algorithm exploiting the variational principle to find the minimal eigenvalue of the given Hamiltonian. A parametrized ansatz function is prepared and measured on the quantum processors, and the parameters are updated via a classical optimizer to minimize the expectation value.

To run the VQE algorithm on quantum processors, a fermionic-to-qubit mapping is essential. The widely-used encoding schemes include the Jordan-Wigner (JW), parity and

doi:10.6342/NTU202401735

Bravyi-Kitaev (BK) encoding [15, 16]. The three encoding schemes encode the n-spin-orbital systems to n qubits. To reduce the qubit usage for simulations, the qubit-efficient encoding (QEE) [17] is proposed. As the fermionic Hamiltonian is particle-conserving, only configurations that lie in the subspace with the correct electron number will contribute to the expectation value. In the QEE procedure, only particle-conserving configurations are mapped to the qubit states by the one-to-one mapping ε, and the procedure for finding the mapping ε is called 'labeling'. In the default labeling method for QEE, the fermionic states and qubit states are sorted by their decimal number representations and labeled one by one in ascending order.

Using QEE, the qubit usage can be reduced to $O(m \log n)$ for systems with n spin-orbitals and m electrons. However, the Pauli terms in the qubit Hamiltonian of QEE are usually more than those of JW or BK encoding [18]. In this thesis, an alternative labeling method for QEE, the single NQ-string labeling, is proposed aiming to reduce the Pauli terms and keep the qubit usage under the same order as QEE with default labeling method.

The thesis is organized as follows. In Chapter 2, the procedure for solving electronic structure problems using the VQE algorithm is introduced. In Chapter 3, the qubit-efficient encoding is introduced, and the procedure of the single NQ-string labeling is proposed. In Chapter 4, simulation results on diatomic molecules are shown and a discussion is made. Finally, the work is concluded in Chapter 5.

doi:10.6342/NTU202401735

Chapter 2 Solving Electronic Structure Problems with Quantum Computing

2.1 Fermionic Hamiltonian

An important problem of quantum chemistry is to find the eigenvalues E and the eigenfunctions $|\Psi\rangle$ in the time-independent Schrödinger equation

$$H|\Psi\rangle = E|\Psi\rangle. \tag{2.1}$$

After the Born-Oppenheimer approximation is applied, the electronic Hamiltonian of the system can be written as

$$H_{elec} = -\sum_i \frac{\nabla_{r_i}^2}{2} - \sum_{I,j} \frac{Z_I}{|R_I - r_j|} + \sum_{i,j>i} \frac{1}{|r_i - r_j|} + \sum_{I,J>I} \frac{Z_I Z_J}{|R_I - R_J|}, \tag{2.2}$$

where R_I, M_I,and Z_I are the position, mass and atomic number of the Ith nucleus, and r_i is the position of the ith electron. Note that the last term in Eq. (2.2) is a constant since it is independent of r_i. Therefore the term can be temporarily neglected and it will finally

doi:10.6342/NTU202401735

be added to the eigenvalues of the remaining part of H_{elec}.

Taking the second-quantized formulation, one can rewrite the first three terms of H_{elec} as

$$H_f = \sum_{p,q} h_{pq} a_p^\dagger a_q + \frac{1}{2} \sum_{p,q,r,s} h_{pqrs} a_p^\dagger a_q^\dagger a_r a_s, \tag{2.3}$$

where h_{pq} and h_{pqrs} are one-electron and two-electron integrals defined as

$$h_{pq} = \int \Psi_p^*(\mathbf{x})(-\frac{\nabla^2}{2} - \sum_I \frac{Z_I}{|r - R_I|})\Psi_q(\mathbf{x})d\mathbf{x}, \tag{2.4}$$

$$h_{pqrs} = \int \frac{\Psi_p^*(\mathbf{x}_1)\Psi_q^*(\mathbf{x}_2)\Psi_r(\mathbf{x}_2)\Psi_s(\mathbf{x}_1)}{|\mathbf{x}_1 - \mathbf{x}_2|} d\mathbf{x}_1 d\mathbf{x}_2, \tag{2.5}$$

with $\Psi_p(\mathbf{x})$ being the orbitals that are linear combinations of some basis wave functions from a certain basis set. The creation operator $a_p^\dagger$ and annihilation operator a_q in Eq. (2.3) are defined as

$$a_p^\dagger \left| f_{n-1} ..., f_p, ..., f_0 \right\rangle = \delta_{0,f_p} (-1)^{\sum_0^{p-1} f_i} \left| f_{n-1} ..., f_p \oplus 1, ..., f_0 \right\rangle, \tag{2.6}$$

$$a_q \left| f_{n-1} ..., f_q, ..., f_0 \right\rangle = \delta_{1,f_q} (-1)^{\sum_0^{q-1} f_i} \left| f_{n-1} ..., f_q \oplus 1, ..., f_0 \right\rangle. \tag{2.7}$$

A fermionic state represented as a ket vector $|f_{n-1}...f_0\rangle$ denotes the occupation numbers of the spin-orbitals. In the binary vector, 1 and 0 represent the occupied and unoccupied spin-orbital respectively. The extra coefficient is added because of the exchange antisymmetry of fermions.

doi:10.6342/NTU202401735

2.2 Fermionic-to-qubit Encoding

A fermionic-to-qubit encoding is a mapping from the fermionic space to the qubit space. Following [19], the encoding is defined mathematically as an isometry $\mathcal{E} : \mathcal{H}_f \rightarrow \mathcal{H}_q$. To run simulations on quantum processors, one should map the fermionic state $|f\rangle$ to qubit state $|q\rangle$ by $|q\rangle = \mathcal{E}|f\rangle$ and construct the counterpart H_q of the second-quantized Hamiltonian H_f in the qubit space by the restriction $H_q\mathcal{E} = \mathcal{E}H_f$.

2.2.1 Jordan-Wigner Encoding

In the Jordan-Wigner (JW) encoding scheme [15], the occupation information of a fermionic state is directly encoded to the qubit state, that is, the qubit state is exactly the same as the fermionic state, $|q\rangle = |f\rangle$. To construct the qubit Hamiltonian H_q, one must express the creation and annihilation operators in the qubit space. For the JW case,

$$a_p^\dagger \rightarrow I_{n-1} \otimes ... \otimes I_{p+1} \otimes \frac{1}{2}(X_p - iY_p) \otimes Z_{p-1} \otimes .... \otimes Z_0, \tag{2.8}$$

$$a_p \rightarrow I_{n-1} \otimes ... \otimes I_{p+1} \otimes \frac{1}{2}(X_p + iY_p) \otimes Z_{p-1} \otimes .... \otimes Z_0, \tag{2.9}$$

which will satisfy Eq. (2.6) (2.7). Note that the extra coefficient $(-1)^{\sum_0^{q-1} f_i}$ for maintaining antisymmetry is represented by the Pauli Z operators. It can be observed from Eq. (2.8)(2.9) that $O(n)$ single-qubit gates are needed to apply a_{n-1} and $a_{n-1}^\dagger$ operators.

doi:10.6342/NTU202401735

2.2.2 Parity Encoding

The $O(n)$ single-qubit gate counts for a_{n-1} and $a_{n-1}^{\dagger}$ operators in the JW encoding scheme arise from the Pauli Z matrices which are applied to maintain antisymmetry. Therefore, a naive way to escape from this problem is to directly encode the parity information into the state in qubit space, which means the state $|f_{n-1}, ...f_1, f_0\rangle$ will be encoded to $|q_{n-1}, ...q_1, q_0\rangle$ where

$$q_i = \sum_{0}^{i} f_i \pmod 2. \tag{2.10}$$

Such encoding scheme is called the parity encoding. The creation and annihilation operators in the qubit space using the parity encoding are of the form

$$a_p^{\dagger} \to X_{n-1} \otimes ... \otimes X_{p+1} \otimes \frac{1}{2}(X_p - iY_p) \otimes I_{p-1} \otimes .... \otimes I_0. \tag{2.11}$$

$$a_p \to X_{n-1} \otimes ... \otimes X_{p+1} \otimes \frac{1}{2}(X_p + iY_p) \otimes I_{p-1} \otimes .... \otimes I_0, \tag{2.12}$$

The qubit usage for the parity encoding is n for a n-spin-orbital system, which is the same as JW encoding. Note that q_{n-1} will be a fixed number in systems where the electron number is conserved. For the total-spin-restricted case, there will be two q_i with fixed values because the number of spin-up and spin-down electrons is conserved. Therefore, in this case two qubits can be reduced in simulations.

It can be observed from Eq. (2.11)(2.12) that for the a_0 and $a_0^{\dagger}$ operators, $O(n)$ single-qubit gates are needed. This stems from the fact that the occupation information of the mode 0, which is the value of f_0, is contained in all qubits as shown in Eq. (2.10). There-

doi:10.6342/NTU202401735

fore, when f_0 needs to be changed, all q_i need to be changed too.

2.2.3 Bravyi-Kitaev Encoding

The JW and parity encoding schemes are like the two sides of the same coin. One directly maps the occupation information while the parity information is distributed over all qubits, and the other maps the parity information directly while the occupation information is distributed over all qubits. Both encoding schemes need $O(n)$ single-qubit gates for applying a creation or annihilation operator in the worst case.

The Bravyi-Kitaev (BK) encoding [16] is a special encoding that modestly stores the occupation and parity information into qubit states. The qubit usage is n for a n-spin-orbital system, and the number of the single-qubit gate scales as $O(\log n)$ for any creation or annihilation operator. In [20], estimations are made that this advantage starts to appear for systems with more than 30 qubits.

After the qubit Hamiltonian is constructed by the fermionic-to-qubit encoding such as JW, parity or BK encoding, the next step is trying to find the minimum eigenvalue of the qubit Hamiltonian, which corresponds to the ground-state energy of the system.

2.3 Variational Quantum Eigensovler

For the system with Hamiltonian H and the ground-state energy E_{min}, the varitional principle states that for any wavefunction Ψ

$$\langle\Psi| H |\Psi\rangle \geq E_{min}. \tag{2.13}$$

doi:10.6342/NTU202401735

If one can find the Ψ such that the expectation value is minimized, then Ψ will fall into the true ground state $|\Psi_{min}\rangle$.

The variational quantum eigensolver (VQE) is a hybrid quantum-classical algorithm for solving the electronic structure problems. In the procedure of VQE, a parametrized trial wavefunction (ansatz state) $|\Psi(\theta)\rangle$ is prepared by quantum processors and is used to calculate the expectation value of qubit Hamiltonian by single qubit measurements. Classical optimizers are used to tune the parameters θ to minimize the expectation value.

The ansatz function $|\Psi(\theta)\rangle$ has the form

$$|\Psi(\theta)\rangle = U(\theta)\,|\Psi_{ref}\rangle\,. \tag{2.14}$$

There are several types of parametrized circuits (ansatz circuits) $U(\theta)$. One of them is the chemical-inspired ansatzes, such as the unitary coupled cluster singles and doubles (UCCSD) ansatz [12, 21], which is inspired by classical coupled cluster theory. The chemical-inspired ansatzes have the advantage that they finely capture the form of the ground state, but the circuits to construct this type of ansatzes are often too deep to be implemented on NISQ devices.

Another type is hardware-efficient ansatzes [22], which are composed of multiple repeated layers of single-qubit rotation gates and two-qubit gates that aim to achieve entanglement. Hardware-efficient ansatzes can be constructed with much shallower circuits. However, because it is a heuristic search of the ground state over the Hilbert space it spans when undergoing the optimization process, one may stuck in local minimums or encounter

doi:10.6342/NTU202401735

a barren plateau problem [23] when a hardware-efficient ansatz is adopted.

The reference state $|\Psi_{ref})\rangle$ is usually chosen close to the true ground state, for example the Hartree-Fock state.

As the qubit Hamiltonian can be decomposed to a summation of Pauli strings,

$$H_q = \sum_i c_i P_i, \tag{2.15}$$

where P_i is a tensor product of Pauli operators I, X, Y, and Z. To get the expectation value of H_q, single-qubit measurements are made to each Pauli string with respect to the corresponding basis.

$$\langle\Psi(\theta)|\, H_q\, |\Psi(\theta)\rangle = \sum_i c_i \langle\Psi(\theta)|\, P_i\, |\Psi(\theta)\rangle. \tag{2.16}$$

doi:10.6342/NTU202401735

doi:10.6342/NTU202401735

Chapter 3 Single NQ-string Labeling

3.1 Qubit-efficient Encoding

3.1.1 Formulation

In JW, parity and BK encoding scheme, n qubits are needed to encode electronic configurations of systems that have n spin-orbitals (for the parity encoding, two qubits can be reduced as the explanation in section 2.2.) The basis function that spans the n-qubit Hilbert space are mostly non-physical configurations, which has an incorrect number of electrons. Since the second-quantized Hamiltonian is particle-conserving, only configurations of a correct number of electrons will contribute to the expectation value of the Hamiltonian. For example, for a system with n spin-orbitals and m electrons, there are $\binom{n}{m}$ particle-conserving configurations. Using these particle-conserving configurations as part of the basis function to span a smaller space with $N_q = \lceil \log_2 \binom{n}{m} \rceil$ qubits, the ground state will lie in the space and the ground-state energy can be obtained. With qubit-efficient encoding (QEE) [17], one can map the particle-conserving configurations to the computational basis states with N_q qubits.

Fermionic states and qubit states can be expressed by unique decimal numbers. For

doi:10.6342/NTU202401735

a fermionic state $|f_{n-1}, f_{n-2}, ..., f_0\rangle$, its decimal number representation is $\sum_{i=0}^{n-1} f_i 2^i$. In the procedure of QEE, fermionic states and qubit states are sorted by their decimal number representations and labeled in ascending order and a one-to-one mapping ε which maps fermionic states to qubit states $|q_i\rangle = \varepsilon |f_i\rangle$ can be defined. The procedure of creating the mapping ε is called 'labeling' in the thesis.

As the example of JW encoding, the next step is to express the creation and annihilation operators in the qubit space. However, a single creation or annihilation operator will change the number of electrons of a state and will make the state not included in the set of particle-conserving configurations. Therefore, a particle-conserving excitation operator $E_{pq} \equiv a_p^\dagger a_q$ is considered and it can be expressed as (Here $p \geq q$ without loss of generality)

$$E_{pq} |f_{n-1}, ...f_p, ..., f_q, ..., f_0\rangle = \delta_{0,f_p}\delta_{1,f_q}(-1)^{\sum_{q+1}^{p-1} f_i} |f_{n-1}, ...f_p \oplus 1, ..., f_q \oplus 1, ..., f_0\rangle . \tag{3.1}$$

The matrix representation of E_{pq} can be expressed as

$$E_{pq} = \sum_{k,k'} c_{kk'}^{pq} |f_k\rangle \langle f_{k'}| , \tag{3.2}$$

where the coefficients $c_{kk'}^{pq} = \delta_{0,f_p}\delta_{1,f_q}(-1)^{\sum_{q+1}^{p-1} f_i}$ have non-zero value only when $|f_k\rangle$ can be excited to $|f_{k'}\rangle$ by E_{pq}.

With the matrix expression, the excitation operator can be mapped to the qubit space via the mapping ε,

$$\tilde{E}_{pq} = \varepsilon E_{pq} \varepsilon^T = \sum_{k,k'} c_{kk'}^{pq} |q_k\rangle \langle q_{k'}| . \tag{3.3}$$

doi:10.6342/NTU202401735

Since $|q_k\rangle = \bigotimes_{i=0}^{N_q-1} |q_i\rangle$ where $q_i = 0, 1$,

$$\tilde{E}_{pq} = \sum_{k,k'} c_{kk'}^{pq} |q_k\rangle \langle q_{k'}| = \sum_{k,k'} \bigotimes_{i=0}^{N_q-1} c_{kk'}^{pq} T_{kk',i}. \tag{3.4}$$

$T_{kk',i}$ are called entry operators corresponding to $|q_k\rangle \langle q_{k'}|$, which have the following four forms,

$$Q^+ = |1\rangle \langle 0| = \frac{1}{2}(X - iY), \tag{3.5}$$

$$Q^- = |0\rangle \langle 1| = \frac{1}{2}(X + iY), \tag{3.6}$$

$$N^{(0)} = |0\rangle \langle 0| = \frac{1}{2}(I + Z), \tag{3.7}$$

$$N^{(1)} = |1\rangle \langle 1| = \frac{1}{2}(I - Z). \tag{3.8}$$

The tensor product of entry operators is called an NQ-string in the thesis. An excitation operator can be expressed as a summation of NQ-strings and thus can be expanded to a linear combination of Pauli matrices.

The second-quantized Hamiltonian of the form as Eq. (2.3) can be rewritten in the form of excitation operator (Here the anticommutation relation $\{a_p^\dagger, a_q\} = \delta_{pq}$ is used)

$$H_f = \sum_{p,q} h_{pq} E_{pq} + \frac{1}{2} \sum_{p,q,r,s} h_{pqrs} (\delta_{qr} E_{ps} - E_{pr} E_{qs}). \tag{3.9}$$

Applying the map ε, i.e. replacing E_{pq} with $\tilde{E}_{pq}$, which can be expanded to Pauli matrices, a QEE qubit Hamiltonian is constructed and can be used in further calculations.

$$H_q = \sum_{p,q} h_{pq} \tilde{E}_{pq} + \frac{1}{2} \sum_{p,q,r,s} h_{pqrs} (\delta_{qr} \tilde{E}_{ps} - \tilde{E}_{pr} \tilde{E}_{qs}). \tag{3.10}$$

doi:10.6342/NTU202401735

3.1.2 An Example: the CO Molecule

In this subsection, an explicit example is shown to demonstrate QEE. Take the CO molecule under the Daubechies wavelet basis with active space selection [24] for example. The interatomic distance is set to 1.12 Å, a distance near the equilibrium bond length. There are six spin-up and six spin-down spin-orbitals, with both four electrons filled in. Considering the total-spin-restricted case, that is, one can treat the spin-up and spin-down subsystems separately, with both subsystems having six spin-orbitals and four electrons. In this case, there are $\binom{6}{4} = 15$ particle-conserving configurations that need to be considered, and four qubits are enough to encode these 15 states. Using the default labeling method of QEE, the one-to-one correspondence of the fermionic configurations and qubit states are as follows, with ascending order of their decimal number representations,

$$\begin{aligned} |f_5 f_4 f_3 f_2 f_1 f_0\rangle &\rightarrow |q_3 q_2 q_1 q_0\rangle \\ |001111\rangle &\rightarrow |0000\rangle \\ |010111\rangle &\rightarrow |0001\rangle \\ |011011\rangle &\rightarrow |0010\rangle \\ &\vdots \\ |111100\rangle &\rightarrow |1110\rangle\,. \end{aligned} \tag{3.11}$$

Here the arrow '$\rightarrow$' denotes the one-to-one map from fermionic states to qubit states.

Considering an excitation operator $E_{51} = a_5^\dagger a_1$, the states involved in this excitation

doi:10.6342/NTU202401735

are (in the fermionic space),

$$
\begin{aligned}
& a_5^\dagger a_1 \\
& |001111\rangle \Rightarrow |101101\rangle \\
& |010111\rangle \Rightarrow |110101\rangle \\
& |011011\rangle \Rightarrow |111001\rangle \\
& |011110\rangle \Rightarrow -|111100\rangle ,
\end{aligned}
\tag{3.12}
$$

where the double arrow '$\Rightarrow$' denotes the excitation transitions. By Eq. (3.12), E_{51} can be expressed as

$$
\begin{aligned}
E_{51} = & |101101\rangle \langle 001111| + |110101\rangle \langle 010111| \\
& + |111001\rangle \langle 011011| - |111100\rangle \langle 011110|
\end{aligned}
\tag{3.13}
$$

in the fermionic space.

In the qubit space, the corresponding states are

$$
\begin{aligned}
& a_5^\dagger a_1 \\
& |0000\rangle \Rightarrow |0111\rangle \\
& |0001\rangle \Rightarrow |1010\rangle \\
& |0010\rangle \Rightarrow |1100\rangle \\
& |0100\rangle \Rightarrow -|1110\rangle .
\end{aligned}
\tag{3.14}
$$

doi:10.6342/NTU202401735

Then the expression of E_{51} in the qubit space (denoted by $\tilde{E}_{51}$) is

$$\begin{aligned}
\tilde{E}_{51} &= |0111\rangle\langle 0000| + |1010\rangle\langle 0001| + |0010\rangle\langle 1100| - |1110\rangle\langle 0100| \\
&= |0\rangle\langle 0| \otimes |1\rangle\langle 0| \otimes |1\rangle\langle 0| \otimes |1\rangle\langle 0| + |1\rangle\langle 0| \otimes |0\rangle\langle 0| \otimes |1\rangle\langle 0| \otimes |0\rangle\langle 1| \\
&+ |0\rangle\langle 1| \otimes |0\rangle\langle 1| \otimes |1\rangle\langle 0| \otimes |0\rangle\langle 0| - |1\rangle\langle 0| \otimes |1\rangle\langle 1| \otimes |1\rangle\langle 0| \otimes |0\rangle\langle 0| \\
&= N^{(0)} \otimes Q^+ \otimes Q^+ \otimes Q^+ + Q^+ \otimes N^{(0)} \otimes Q^+ \otimes Q^- \\
&+ Q^- \otimes Q^- \otimes Q^+ \otimes N^{(0)} - Q^+ \otimes N^{(1)} \otimes Q^+ \otimes N^{(0)},
\end{aligned} \tag{3.15}$$

which is a summation of NQ-strings. One can expand the NQ-string to write $\tilde{E}_{51}$ in summation of Pauli strings by the definitions of entry operators. After computing all excitation operators, the qubit Hamiltonian can be constructed with Eq. (3.10).

3.1.3 Problems of QEE

Although there is exponential reduction ($N_q = O(m \log n)$) of qubit usage using QEE, problems about the large number of Pauli terms in qubit Hamiltonian emerge. Take the example of the CO molecule in section 3.1.2, the number of Pauli terms in the QEE qubit Hamiltonian is 15648. As a comparison, the number of Pauli terms in the 12-qubit Hamiltonian is 831 using JW encoding.

The QEE qubit Hamiltonian is constructed by entry operators. All entry operators are linear combinations of two Pauli operators. The N operators, $N^{(0)}$ and $N^{(1)}$, are composed of I, Z, and the Q operators, Q^+ and Q^-, are composed of X, Y. Therefore, a single NQ-string (for example $N^{(0)}Q^+Q^-Q^+$) will be expanded to a summation of 2^l Pauli strings, where l is the length of the NQ-string.

doi:10.6342/NTU202401735

In a system of n spin-orbitals and m electrons, $l = \lceil \log_2 \binom{n}{m} \rceil$. For all the excitation operators E_{pq}, except for the two spin-orbitals p and q and the electron involved in the excitation, there are $n-2$ spin-orbitals and $m-1$ electrons remaining. Therefore $\binom{n-2}{m-1}$ pairs of configurations will be involved in the excitation and will contribute to the expression of E_{pq}.

By the above discussion, a single excitation operator will be expanded to

$$\binom{n-2}{m-1} * 2^{\lceil \log_2 \binom{n}{m} \rceil} = O(\frac{n^{2m-1}}{(m-1)!m!}) \tag{3.16}$$

Pauli terms.

In general, the more Pauli terms in the Hamiltonian, the more quantum resources are needed to run quantum algorithms. The large number of Pauli terms will decrease the efficiency of running simulations. In the next section, a different labeling method, which is called single NQ-string labeling for QEE, is proposed that aims to systematically reduce the Pauli terms in the qubit Hamiltonian.

3.2 Single NQ-string Labeling

3.2.1 Motivation

To reduce the Pauli terms in the qubit Hamiltonian, one possible approach is to reduce the Pauli terms of the excitation operators $\tilde{E}_{pq}$. According to Eq. (3.15) in section 3.1.2, $\tilde{E}_{51}$ is expanded to 64 Pauli terms. This is because the four NQ-string are all distinct, so they are expanded to distinct Pauli strings. An intuitive way to reduce the number of terms

doi:10.6342/NTU202401735

is to make all the NQ-strings the same by rearranging the labels.

Take the $\tilde{E}_{51}$ of the CO molecule as an example again. The goal is to arrange the labels of states involving the excitation so that it can be expressed as

$$\tilde{E}_{51} = \sum_{i=1}^{4} T_i^{(1)} \otimes T_i^{(2)} \otimes T_i^{(3)} \otimes T_i^{(4)}, \tag{3.17}$$

where $\forall j,\ \forall i\ T_i^{(j)} \in \{N^{(0)}, N^{(1)}\}\ \vee\ \forall i\ T_i^{(j)} \in \{Q^+, Q^-\}$. That is, in general each of the four $T_i^{(1)}$ in the summation could be either an N operator or a Q operator, and so as four $T_i^{(2)}$, four $T_i^{(3)}$, and four $T_i^{(4)}$.

If one can use some efficient labeling method to label each excitation operator $\tilde{E}_{pq}$ in only a single NQ-string, then when expanding the NQ-strings into Pauli operators, one can combine the same Pauli strings together to reduce the number of the Pauli terms in the Hamiltonian. In Eq. (3.17), if $\forall i\ T_i^{(1)} \in \{N^{(0)}, N^{(1)}\}$ and $\forall i\ T_i^{(j)} \in \{Q^+, Q^-\},\ j = 2, 3, 4$, then in this case, $\tilde{E}_{51}$ can be cast into a single NQ-string expression of $NQQQ$. Such a labeling method is named 'single NQ-string labeling' in this thesis. In the following, we will discuss how to achieve the single NQ-string labeling for the excitation operators.

3.2.2 Procedure

The procedure for the single NQ-string labeling is as follows:

(Step 1) Calculate the qubit number needed to satisfy the single NQ-string constraint.

(Step 2) Generate a dictionary and give each excitation operator a single NQ-string ex-

doi:10.6342/NTU202401735

pression under the constraint to ensure the encoding of states.

(Step 3) Give the Hartree-Fock state the label $|00..0\rangle$ in the qubit space and obtain other states' labels via the dictionary generated in step 2.

The details of the procedure will be explained in the following sections.

3.2.3 Qubit Number Calculation

Requiring that all excitation operators be in the form of a single NQ-string will reduce the number of Pauli terms. However, the qubit usage may increase because of the extra constraint. In this section, a calculation of the qubit number needed in the single NQ-string labeling will be made.

3.2.3.1 Properties of Single NQ-string Expressions for Excitation Operators

By the definition of excitation operators, the following properties will hold:

(1) $\tilde{E}_{pq}$ with $p = q$ has the single NQ-string expression of $N...NN$.

(2) If $\tilde{E}_{pq}$ has a single NQ-string expression, then $\tilde{E}_{qp}$ will have the same NQ-string expression.

(3) If $\tilde{E}_{pq}$ has the single NQ-string expression of $T_1T_2...T_n$, and $\tilde{E}_{qr}$ has the single NQ-string expression of $S_1S_2...S_n$, then $\tilde{E}_{pr} = \tilde{E}_{pq} * \tilde{E}_{qr}$ has the single NQ-string ex-

doi:10.6342/NTU202401735

pression of $(T_1 * S_1)(T_2 * S_2)...(T_n * S_n)$, where the $*$ operation is defined as

$$Q * Q = N * N = N,$$
$$Q * N = N * Q = Q. \tag{3.18}$$

3.2.3.2 Single NQ-string Constraint

A successful single NQ-string labeling must satisfy the following constraint:

* For a system with m electrons (assume $m \leq \frac{n}{2}$ for convenience), any combination of $i \leq m$ different excitation operators with distinct indices cannot have the single NQ-string expression of $N...NN$.

Two excitation operators $\tilde{E}_{ab}$ and $\tilde{E}_{cd}$ are with distinct indices if all the indices a, b, c and d are distinct. For a system with m electrons, any transition between two physical configurations can be achieved by at most m excitation operators with distinct indices. To prevent giving different states the same label, the constraint needs to be satisfied. For example, $\tilde{E}_{01} * \tilde{E}_{23} * \tilde{E}_{45}$ cannot have the expression of $N...NN$ in a system with six spin-orbitals and three electrons, otherwise $|010101\rangle$ and $|101010\rangle$ will be given the same label in the qubit space.

3.2.3.3 Qubit Number Needed

For a system having n spin-orbitals, there are $2\binom{n}{2}$ excitation operators $\tilde{E}_{pq}$ with $p \neq q$. Therefore, $\binom{n}{2}$ single NQ-string expressions are needed to give to these excitation operators since under our consideration $\tilde{E}_{pq}$ and $\tilde{E}_{qp}$ have the same expression (for conve-

doi:10.6342/NTU202401735

nience they are regarded as the same in the following discussion). By the third property in section 3.2.3.1, we can use a pool of $n-1$ excitation operators $\{\tilde{E}_{01}, \tilde{E}_{02}, \tilde{E}_{03}..., \tilde{E}_{0,n-1}\}$ to represent the $\binom{n}{2}$ excitation operators, since excitation operators that are not in the pool can be generated by the combination of two of them in the pool.

With the constraint described in section 3.2.3.2, since an excitation operator may be a combination of two excitation operators in the pool, the constraint becomes that any combination of $i \leq 2m$ excitation operators in the pool cannot have the single NQ-string expression of $N...NN$. Therefore, for the excitation operator $\tilde{E}_{0,n-1}$ in the pool, its single NQ-string expression must be different from any combination of $i \leq 2m-1$ excitation operators in the pool. By discussion above, the single NQ-string expression of $\tilde{E}_{0,n-1}$ must be distinct to

$$\binom{n-2}{1} + \binom{n-2}{2} + ... + \binom{n-2}{2m-1} = \sum_{i=1}^{2m-1} \binom{n-2}{i} \tag{3.19}$$

expressions. Note that for the special case $n = 2m$, there is no $\binom{n-2}{2m-1}$ term, so the term is discarded in this case, and the summation can be rewritten as

$$\sum_{i=1}^{\min\{2m-1,n-2\}} \binom{n-2}{i}. \tag{3.20}$$

There are 2^l different NQ-strings with length l, therefore the qubit number needed for single NQ-string labeling is

$$N_q = \lceil \log_2 (\sum_{i=1}^{\min\{2m-1,n-2\}} \binom{n-2}{i} + 2) \rceil. \tag{3.21}$$

where the $+2$ in Eq. (3.21) denotes the single NQ-string expression of itself and the ex-

doi:10.6342/NTU202401735

pression of $N...NN$ that cannot be used in $\tilde{E}_{pq}$ with $p \neq q$. In the limit $n \gg m$, the qubit usage is of order $O(m \log n)$, which is the same as QEE with default encoding.

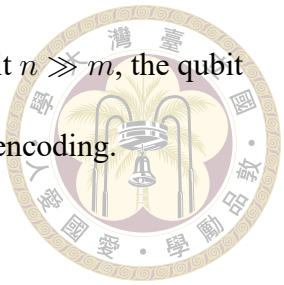

3.2.4 Generation of the Dictionary and the State Labeling

After the qubit number needed is calculated, the next step of the single NQ-string labeling is generating the dictionary that gives each excitation operator a single NQ-string expression. Following the discussion in 3.2.3.3, the task is equivalent to giving a single NQ-string expression to the $n-1$ excitation operators in the pool $\{\tilde{E}_{01}, \tilde{E}_{02}, \tilde{E}_{03}..., \tilde{E}_{0,n-1}\}$ under the constraint in section 3.2.3.2.

After giving the first element in the pool, $\tilde{E}_{01}$, an arbitrary single NQ-string expression of length N_q, the pool can be generated iteratively by giving excitation operators single NQ-string expressions and adding to the pool one by one. Every new excitation operator to be added to the pool must have the single NQ-string expression that satisfies the constraints.

After giving each excitation operator a single NQ-string expression, the final step of the single NQ-string labeling is to label the states. In the VQE simulation for the ground-state energy, the Hartree-Fock state is often picked as the reference state of the parametrized wavefunction. The quantum register is usually initialized to $|0\rangle$; therefore, labeling the Hartree-Fock state to $|0..000\rangle$ in the qubit space will be a convenient choice since no extra gates are needed to prepare the reference state on quantum processors. With the generated dicitonary of single NQ-string expressions for excitation operators, the labels of other states can be determined.

doi:10.6342/NTU202401735

3.2.5 An example: A System with Six Spin-orbitals and Three Electrons

In this section, an explicit sample will be given to demonstrate the procedure of the single NQ-string labeling method. For the system with six spin-orbitals and three electrons, the first step is calculating the qubit usage by Eq. (3.21):

$$\begin{aligned} N_q &= \lceil \log_2 \sum_{i=1}^{4} \binom{4}{i} + 2 \rceil \\ &= 5. \end{aligned} \tag{3.22}$$

The next step is to give each excitation operator in the pool $\{\tilde{E}_{01}, \tilde{E}_{02}, \tilde{E}_{03}, \tilde{E}_{04}, \tilde{E}_{05}\}$ a single NQ-string expression. There are multiple choices of the expressions, here for simplicity, we can assign

$$\begin{cases} \tilde{E}_{01} : \ NNNNQ \\ \tilde{E}_{02} : \ NNNQN \\ \tilde{E}_{03} : \ NNQNN \\ \tilde{E}_{04} : \ NQNNN \\ \tilde{E}_{05} : \ QNNNN. \end{cases} \tag{3.23}$$

It is easy to check that the five excitation operators in the pool satisfy the constraint. That is, any combinations of one, two, three, four, and five excitation operators in the pool do not have the single NQ-string expression of $N...NN$.

As for the state labeling, we start by assigning the Hartree-Fock state $|000111\rangle$ to $|00000\rangle$ in the qubit space, and then with the dictionary, we can label the states that can be

doi:10.6342/NTU202401735

transformed from $|000111\rangle$ by a single excitation operator. For example, state $|100110\rangle$ can be obtained by acting E_{50} on $|000111\rangle$. As $\tilde{E}_{50}$, which is the counterpart of E_{50} in the qubit space, has the expression of $QNNNN$ as shown in Eq. (3.23), we label fermionic state $|100110\rangle$ to qubit state $|10000\rangle$ to satisfy the expression. Repeat the procedure until all physical configurations are given labels, and then the labeling process is completed.

3.2.6 Number of Pauli Terms

In section 3.2.3.3, the qubit number needed for the single NQ-string labeling is calculated as Eq. (3.21). Therefore, an excitation operator $\tilde{E}_{pq}$ will be expanded to

$$2^{N_q} = 2^{\lceil \log_2 (\sum_{i=1}^{\min\{2m-1,n-2\}} \binom{n-2}{i}+2)\rceil} = O(\frac{n^{2m-1}}{(2m-1)!}) \tag{3.24}$$

Pauli terms. The asymptotic number of Pauli terms using QEE with two labeling methods are listed in Table 3.1. The number of Pauli terms is reduced by the $\frac{(2m-1)!}{m!(m-1)!} = \binom{2m-1}{m}$ multiplier, which is an exponential reduction with respect to the electron number m. However, QEE works better in the case $n \gg m$, and the $n^{(2m-1)}$ will dominate the number of Pauli terms. Therefore the term reduction is limited asymptotically. For small systems, the effectiveness of the term reduction may be more evident and will be shown in the next chapter by running simulations of some diatomic molecules.

labeling method	default	single NQ-string
Pauli term number of single excitation opertor	$O(\frac{n^{2m-1}}{(m-1)!m!})$	$O(\frac{n^{2m-1}}{(2m-1)!})$

Table 3.1: Order of the Pauli term number for single excitation operator using different labeling method

doi:10.6342/NTU202401735

Chapter 4 Results

4.1 Number of Pauli Terms for Hamiltonian of Diatomic Molecules

To test the effectiveness of Pauli-term reduction of single-NQ string labeling, ten diatomic molecules are chosen for calculation, the results are shown in Table 4.1. All the qubit Hamiltonians are generated in the Daubechies wavelet basis with active space selection [24], and the total-spin-restricted case is considered. The interatomic distances of the molecules are set to their equilibrium bond lengths. Note that the parity encoding is performed with 2-qubit reduction because of the number conservation of spin-up and spin-down electrons.

For the LiBr and BeO molecules, the qubit usage of QEE and the parity encoding is the same, and the Pauli term number of parity is much less than that of QEE with both default labeling and single NQ-string labeling. Therefore, systems with five spin-orbitals and three electrons, as well as systems with six spin-orbitals and three electrons for spin-up and spin-down cases respectively are not suitable for the QEE scheme. The result meets our expectations since for both cases the spin-orbitals are near half-filled.

doi:10.6342/NTU202401735

Molecule	LiBr	LiF	SiSe	GeO	CO
Spin-orbitals Electrons	(5,5) (3,3)	(6,6) (2,2)	(6,6) (4,4)	(6,6) (4,4)	(6,6) (4,4)
Qubit usage (QEE default)	8	8	8	8	8
Number of Pauli terms (QEE default)	8737	16128	15000	14952	15596
Qubit usage (QEE Single NQ)	8	8	8	8	8
Number of Pauli terms (QEE Single NQ)	2792	4528	2226	2140	2736
Qubit usage (parity)	8	10	10	10	10
Number of Pauli terms (parity)	400	935	883	871	831

Molecule	BCl	Br_2	BeO	BH	Cl_2
Spin-orbitals Electrons	(6,6) (4,4)	(6,6) (4,4)	(6,6) (3,3)	(7,7) (2,2)	(7,7) (5,5)
Qubit usage (QEE default)	8	8	10	10	10
Number of Pauli terms (QEE default)	14912	16504	109067	225036	173064
Qubit usage (QEE Single NQ)	8	8	10	10	10
Number of Pauli terms (QEE Single NQ)	1964	2888	8078	61214	43450
Qubit usage (parity)	10	10	10	12	12
Number of Pauli terms (parity)	807	851	915	1982	1686

Table 4.1: Number of qubit usage and Pauli terms using QEE (default), QEE (single NQ) and the parity encoding schemes for ten diatomic molecules. The (,) in the row 'spin-orbitals' and 'electrons' denotes the number of spin-up and spin-down spin-orbitals and electrons.

doi:10.6342/NTU202401735

For the other eight molecules in Table 4.1, two qubits can be reduced using QEE compared to the parity encoding. Considering the computational time cost, systems that need more than eight qubits will not be chosen to run simulations. Under this consideration, systems with six spin-orbitals and two (or four) electrons for spin-up and spin-down cases respectively, which need eight qubits for simulations, are the suitable choices. There are six molecules in Table 4.1 with this size of spin-orbitals and electrons, and the Pauli terms in the Hamiltonians of these molecules can be reduced at least by a factor of 3.5 (which is the LiF case). Among the six molecules, the SiSe, GeO, and CO molecules are picked to run VQE simulations as simulations on these three molecules with the parity encoding are made in [24], and the results can be put in comparison.

4.2 VQE Simulation Results

For the VQE simulations, the hardware-efficient RealAmplitude ansatz circuit is adopted. Take the eight-qubit system for example, in each layer of the ansatz circuit, there is a layer of rotational-Y gates with tunable parameters θ_i acting on all qubits, then followed by seven CNOT gates of the nearest neighbor. The circuit depth of the first layer is eight, and the circuit depth will increase by three after a repeated layer is added, as gates in adjacent layers on the circuit are arranged as shown in Figure 4.1. At the end of the ansatz circuit, an extra layer of rotational-Y gates is added to each qubit and this causes the circuit depth to increase by one. According to the discussion, the circuit depth for the whole RealAmplitude ansatz of q qubits with repetition of layers r has the depth $3r+q-2$, and the number of tunable parameters is $q*(r+1)$.

doi:10.6342/NTU202401735

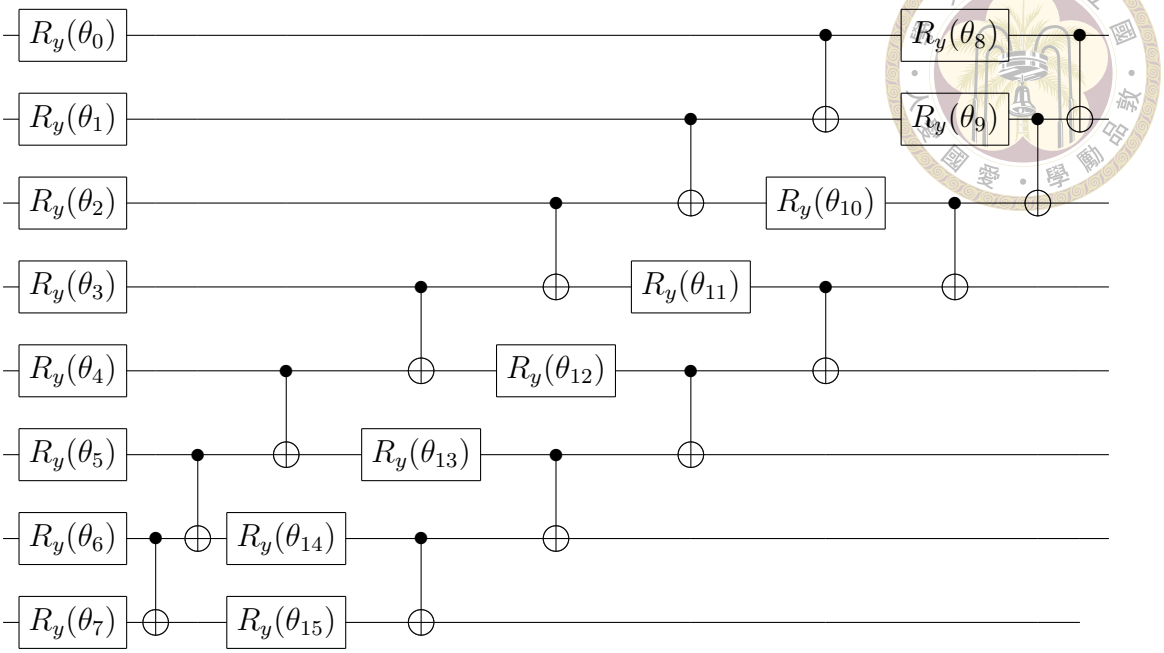

Figure 4.1: Two layers of an eight-qubit RealAmplitude ansatz with reverse-linear entanglement pattern.

In the simulation of the 8-qubit system, the repetition of layers is set to 15 in order to improve the expressibility of the ansatz states. The Hartree-Fock state, which is $|0\rangle^{\otimes Q}$ in the qubit space for QEE with both labeling methods, is chosen as the reference state and thus no extra single-qubit gate is needed to prepare the state. The initial parameters for the rotational-Y gates in the ansatz circuit are set to random numbers that are uniformly sampled in the interval $[-0.1, 0.1]$.

The quantum circuit generations and the expectation value calculations are done on the Qiskit platform. Especially, the expectation values are calculated by the noiseless Qiskit Aer Estimator. The L-BFGS-B optimizer is chosen to minimize the expectation value.

doi:10.6342/NTU202401735

4.2.1 QEE Default v.s. QEE Single NQ-string

For the three molecules, five interatomic distances around their equilibrium bond length are picked to run a two-round VQE simulation, which is a method inspired by [24]. In the first round, the initial parameters of the ansatz circuit for the five interatomic distances are set to different random numbers sampled from the interval $[-0.1, 0.1]$. For the second-round VQE, the initial parameters are set as the optimal parameters for the point that the energy is closest to the exact energy in the first-round VQE.

The second-round VQE results of the potential energy surfaces and the energy errors compared to the exact diagonalization results are shown in Figures 4.2, 4.3 and 4.4. Note that for the simulations for the single NQ-string labeling, the two-round VQE is executed once. While for the default labeling case, two-round VQE simulations are made four times with different sets of the random initial parameters. The results presented in Figures 4.2, 4.3 and 4.4 are the results that obtain the smallest summations of errors of energies for the five interatomic distances compared to the exact diagonalization results.

For the three molecules, the energy errors for both labeling methods are within the chemical accuracy, which is $1 kcal/mol$. Also, it can be observed that the converged energies of QEE with the single NQ-string labeling are generally lower than those of QEE with default labeling under the same settings of the initial ansatz circuits composed of 15 repeated layers.

For the Hamiltonian composed of more Pauli terms, the optimization for the parameters of the ansatz circuits may be more difficult. As the expectation values are calculated

doi:10.6342/NTU202401735

Molecule \ Method	QEE Single NQ	QEE Default
CO	6769 + 4149	48981 + 25706
GeO	3564 + 5187	24171 + 22158
SiSe	8321 + 3982	20143 + 16752

Table 4.2: The optimization time (in second) of two-round VQE simulations for three molecules with two labeling methods for QEE.

by $\sum_i c_i \langle \Psi(\theta)| P_i |\Psi(\theta)\rangle$, the adjustments on parameters will be affected by more terms in the summation in the optimization process. This may explain why the results of the converged energies obtained by the single NQ-string labeling are better than those by the default labeling.

It is expected that the optimization time using the single NQ-string labeling will be less than that of the default labeling because of the Pauli-term reduction in the qubit Hamiltonian. The results of optimization time for the two-round VQE are shown in Table 4.2. Note that the VQE with five different interatomic distances are run simultaneously, therefore the overall optimization time is determined by the longest time among the runtimes of the five points.

For the default labeling case, if one wants to obtain a similar accuracy to the single NQ-string labeling case, the number of repeated layers in ansatz circuits may need to increase and the time costs for the optimization process will even increase.

From the above results, QEE with the single NQ-string labeling can achieve better energies in shorter times than the correspondent QEE with the default labeling. Therefore, for a system that has an active space with six spin-orbitals and two (or four) electrons, the single NQ-string labeling is the preferred labeling method for QEE in VQE simulations.

doi:10.6342/NTU202401735

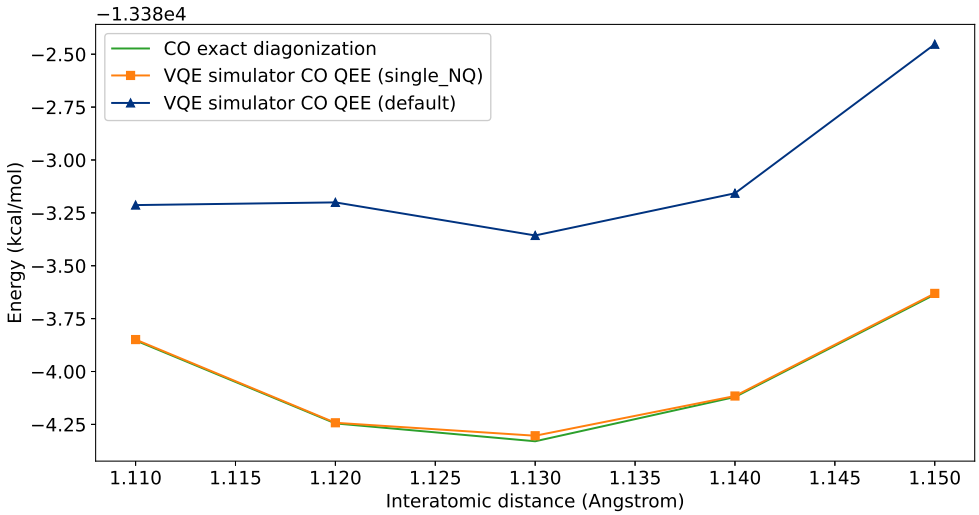

(a)

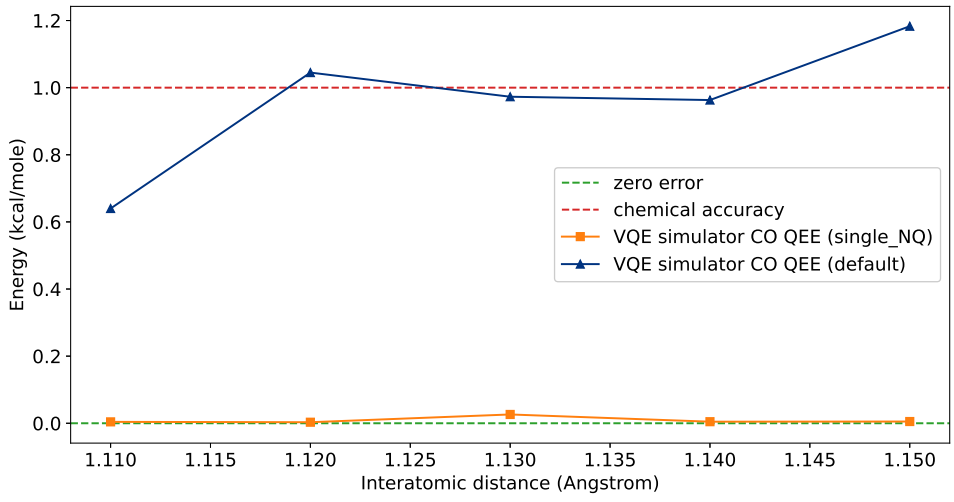

(b)

Figure 4.2: (a) Potential energy curves and (b) energy errors of CO molecule with two labeling methods. The dashed red line in (b) is the line denoting the chemical accuracy, 1 kcal/mol.

doi:10.6342/NTU202401735

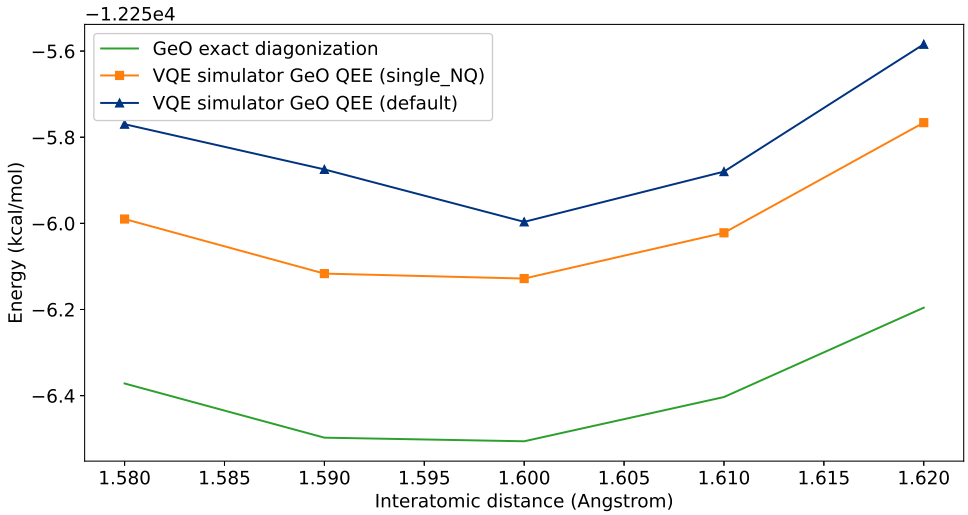

(a)

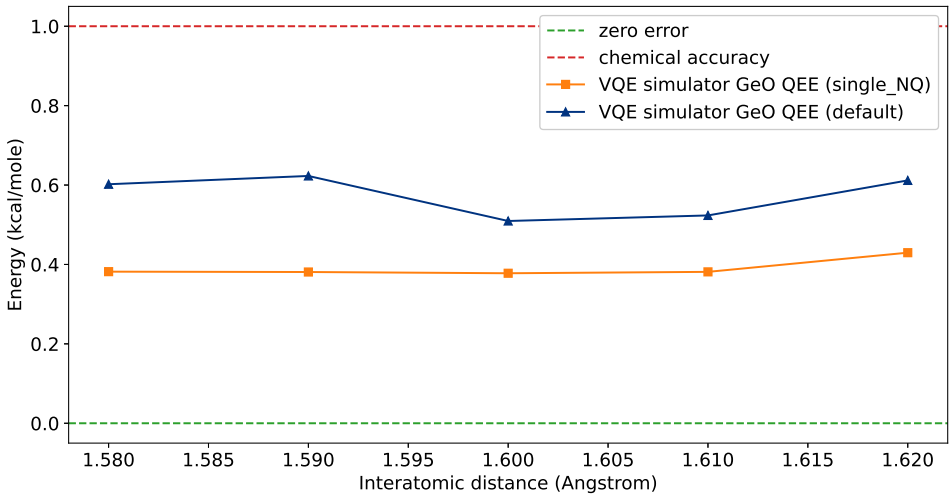

(b)

Figure 4.3: (a) Potential energy curves and (b) energy errors of GeO molecule with two labeling methods. The dashed red line in (b) is the line denoting the chemical accuracy, 1 kcal/mol.

doi:10.6342/NTU202401735

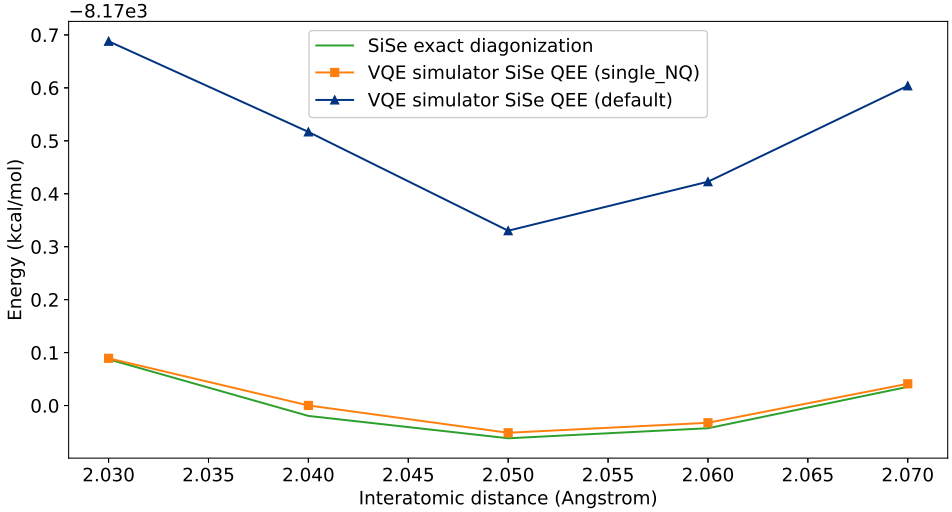

(a)

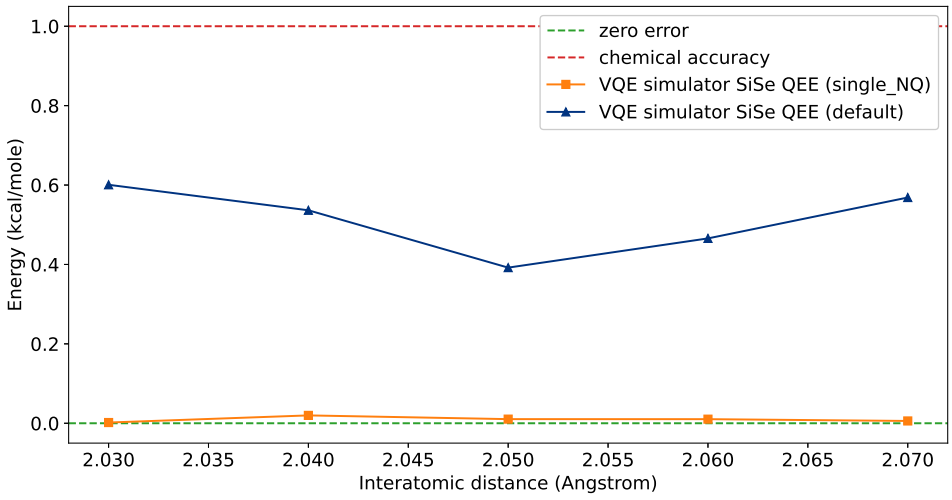

(b)

Figure 4.4: (a) Potential energy curves and (b) energy errors of SiSe molecule with two labeling methods. The dashed red line in (b) is the line denoting the chemical accuracy, 1 kcal/mol.

doi:10.6342/NTU202401735

4.2.2 QEE Single NQ-string v.s. Parity

Besides the ground-state energy, the harmonic vibrational frequency is also an important physical quantity. With five data points near the equilibrium bond length, the harmonic vibrational frequency can be obtained by quadratic curve-fitting on the data points. Unlike the energy simulation, to get accurate vibrational frequencies, all data points should have similar energy accuracies, and this is the reason why the two-round VQE method is taken. With the same initial parameters that are good enough to capture the ground state near the equilibrium bond length, for the second-round VQE it is believed that all data points will reach similar accuracy.

In this section, the results of harmonic vibrational frequencies using QEE with the single NQ-string labeling are compared with the results of [24] as shown in Table 4.3. The errors compared to the exact diagonalization results for the three molecules using QEE with the single NQ-string labeling are much larger than those of the simulation results using the parity encoding. Trying to obtain better accuracies for the harmonic vibrational frequencies, besides adjusting the number of repeated layers of the ansatz or the settings for optimization such as the type of optimizers, there is another way to explore only when the single NQ-string labeling for QEE is adopted, which is the degree of freedom of the qubit Hamiltonian. The following discussion is about how to make use of this degree of freedom.

In the above VQE simulations using QEE with the single NQ-string labeling, a fixed pool of the excitation operators is used, and the single NQ-string expressions of the exci-

doi:10.6342/NTU202401735

Molecule \ Method	QEE Single NQ	Parity	Exact
CO	2219.31 (-0.97%)	2249.18 (0.31%)	2242.16
GeO	1065.00 (6.53%)	1012.25 (1.26%)	999.63
SiSe	567.28 (-4.21%)	584.19 (-1.36%)	592.24

Table 4.3: Harmonic vibrational frequencies (in cm^{-1}) for three molecules for QEE with the single NQ-string labeling and the parity encoding. The percentages in parentheses are the relative errors compared to the exact diagonalization results.

tation operators in the pool are as follows:

$$\begin{cases} \tilde{E}_{01} : NNNQ \\ \tilde{E}_{02} : NNQN \\ \tilde{E}_{03} : NQNN \\ \tilde{E}_{04} : QNNN \\ \tilde{E}_{05} : QQQQ. \end{cases} \tag{4.1}$$

The single NQ-string expressions satisfy the constraint mentioned in section 3.2.3.2 since any combinations of one, two, three, and four excitation operators in the pool will not have the expression of $N...NN$. In fact, the choice of the single NQ-string expressions can be arbitrary as long as the constraint is satisfied.

Following this point, a slight change in the two-round VQE procedure is made. Besides the different random initial parameters sampled from the interval $[-0.1, 0.1]$, the Hamiltonians in the first-round VQE are generated with different random expressions for five interatomic distances. Then in the second round of VQE simulations, the Hamiltonians and initial parameters of the five data points are set the same as the Hamiltonian and optimal parameters that obtain the closest energy to the exact diagonalization result

doi:10.6342/NTU202401735

Molecule \ Method	QEE Single NQ (random H.)	Parity	Exact
CO	2242.48 (0.01%)	2249.18 (0.31%)	2242.16
GeO	1011.35 (1.17%)	1012.25 (1.26%)	999.63
SiSe	602.07 (1.66%)	584.19 (-1.36%)	592.24

Table 4.4: Harmonic vibrational frequencies (in cm^{-1}) for three molecules for QEE with the single NQ-string labeling (with random Hamiltonian) and the parity encoding. The percentages in parentheses are the relative errors compared to the exact diagonalization results.

among the data points in the first round. In this setting of random initial Hamiltonian, the results are shown in Table 4.4. With the random Hamiltonian setting, results of similar or even better precision compared to the results of the parity encoding can be obtained.

There may be Hamiltonian that the true ground state is easier to be approached with certain internal structures of ansatz circuits. In other words, for the RealAmplitude ansatz with inverse linear entanglement pattern which is used for simulations in this thesis, there may exist a Hamiltonian that its true ground state can be easily approached by this ansatz in the optimization procedure. This could be the reason why after the degree of freedom of the initial Hamiltonian is added, better results are obtained in VQE simulations for the three molecules.

For simulations using the parity encoding, ten qubits are used and the number of repeated layers of RealAmplitude ansatz is 25 or 30, compared to eight qubits and 15 repeated layers that are used in simulations of QEE with the single NQ-string labeling.

With fewer qubits, and shallower circuit depth to get the results with similar precision, QEE with the single NQ-string labeling is a preferred choice over the parity encoding.

doi:10.6342/NTU202401735

Chapter 5 Conclusion

For systems with n spin-orbitals and m electrons, the qubit usage for VQE simulations can be reduced to $O(m \log n)$ using the qubit-efficient encoding. However, the large number of Pauli terms in the QEE qubit Hamiltonian increases the computational resources and time costs for simulations. Trying to relieve the problem, an alternative labeling method for QEE, the single NQ-string labeling, is proposed in this thesis. By requiring that all excitation operators be the expression of a single NQ-string, a qubit Hamiltonian can be constructed with the same order of qubit usage, $O(m \log n)$ as the default labeling method in QEE. At the same time, there is an exponential reduction of Pauli terms with respect to the electron number m. However, the effect of reducing the number of Pauli terms using the single NQ-string labeling is limited asymptotically as QEE works better in the $n \gg m$ case.

To test the effectiveness of the single NQ-string labeling for smaller systems, three diatomic molecules in the Daubechies wavelet basis set with active space selection are chosen to run VQE simulations. For the three molecules, there are six spin-orbitals and four electrons for both spin-up and spin-down cases, and therefore eight qubits are needed for simulations. Desirable results about the ground-state energies and the harmonic vibra-

doi:10.6342/NTU202401735

tional frequencies can be obtained by the two-round VQE procedure with random initial Hamiltonian. Moreover, the quantum resources and optimization time costs are reduced compared to the existing encoding methods.

doi:10.6342/NTU202401735

References

[1] Richard P. Feynman. Simulating physics with computers. International Journal of Theoretical Physics, 21(6):467–488, Jun 1982.

[2] Bela Bauer, Sergey Bravyi, Mario Motta, and Garnet Kin-Lic Chan. Quantum algorithms for quantum chemistry and quantum materials science. Chemical Reviews, 120(22):12685−12717, October 2020.

[3] Jiangfeng Du, Nanyang Xu, Xinhua Peng, Pengfei Wang, Sanfeng Wu, and Dawei Lu. NMR implementation of a molecular hydrogen quantum simulation with adiabatic state preparation. Physical Review Letters, 104:030502, Jan 2010.

[4] Zhaokai Li, Man-Hong Yung, Hongwei Chen, Dawei Lu, James D. Whitfield, Xinhua Peng, Alán Aspuru-Guzik, and Jiangfeng Du. Solving quantum ground-state problems with nuclear magnetic resonance. Scientific Reports, 1(1), September 2011.

[5] B. P. Lanyon, J. D. Whitfield, G. G. Gillett, M. E. Goggin, M. P. Almeida, I. Kassal, J. D. Biamonte, M. Mohseni, B. J. Powell, M. Barbieri, A. Aspuru-Guzik, and A. G. White. Towards quantum chemistry on a quantum computer. Nature Chemistry, 2(2):106−111, January 2010.

doi:10.6342/NTU202401735

[6] S. Paesani, A. A. Gentile, R. Santagati, J. Wang, N. Wiebe, D. P. Tew, J. L. O'Brien, and M. G. Thompson. Experimental Bayesian quantum phase estimation on a silicon photonic chip. Physical Review Letters, 118:100503, Mar 2017.

[7] Raffaele Santagati, Jianwei Wang, Antonio A. Gentile, Stefano Paesani, Nathan Wiebe, Jarrod R. McClean, Sam Morley-Short, Peter J. Shadbolt, Damien Bonneau, Joshua W. Silverstone, David P. Tew, Xiaoqi Zhou, Jeremy L. O' Brien, and Mark G. Thompson. Witnessing eigenstates for quantum simulation of Hamiltonian spectra. Science Advances, 4(1):eaap9646, 2018.

[8] Ian D. Kivlichan, Jarrod McClean, Nathan Wiebe, Craig Gidney, Alán Aspuru-Guzik, Garnet Kin-Lic Chan, and Ryan Babbush. Quantum simulation of electronic structure with linear depth and connectivity. Physical Review Letters, 120:110501, Mar 2018.

[9] Sam McArdle, Suguru Endo, Alán Aspuru-Guzik, Simon C. Benjamin, and Xiao Yuan. Quantum computational chemistry. Reviews of Modern Physics, 92(1), March 2020.

[10] John Preskill. Quantum computing in the NISQ era and beyond. Quantum, 2:79, August 2018.

[11] Kishor Bharti, Alba Cervera-Lierta, Thi Ha Kyaw, Tobias Haug, Sumner Alperin-Lea, Abhinav Anand, Matthias Degroote, Hermanni Heimonen, Jakob S. Kottmann, Tim Menke, Wai-Keong Mok, Sukin Sim, Leong-Chuan Kwek, and Alán Aspuru-Guzik. Noisy intermediate-scale quantum algorithms. Reviews of Modern Physics, 94(1), February 2022.

doi:10.6342/NTU202401735

[12] Alberto Peruzzo, Jarrod McClean, Peter Shadbolt, Man-Hong Yung, Xiao-Qi Zhou, Peter J. Love, Alán Aspuru-Guzik, and Jeremy L. O' Brien. A variational eigenvalue solver on a photonic quantum processor. Nature Communications, 5(1), July 2014.

[13] P. J. J. O'Malley, R. Babbush, I. D. Kivlichan, J. Romero, J. R. McClean, R. Barends, J. Kelly, P. Roushan, A. Tranter, N. Ding, B. Campbell, Y. Chen, Z. Chen, B. Chiaro, A. Dunsworth, A. G. Fowler, E. Jeffrey, E. Lucero, A. Megrant, J. Y. Mutus, M. Neeley, C. Neill, C. Quintana, D. Sank, A. Vainsencher, J. Wenner, T. C. White, P. V. Coveney, P. J. Love, H. Neven, A. Aspuru-Guzik, and J. M. Martinis. Scalable quantum simulation of molecular energies. Physical Review X, 6:031007, Jul 2016.

[14] Dmitry A. Fedorov, Bo Peng, Niranjan Govind, and Yuri Alexeev. VQE method: A short survey and recent developments, 2021.

[15] P. Jordan and E. Wigner. Über das Paulische äquivalenzverbot. Zeitschrift für Physik, 47(9):631–651, Sep 1928.

[16] Sergey B. Bravyi and Alexei Yu. Kitaev. Fermionic quantum computation. Annals of Physics, 298(1):210–226, 2002.

[17] Yu Shee, Pei-Kai Tsai, Cheng-Lin Hong, Hao-Chung Cheng, and Hsi-Sheng Goan. Qubit-efficient encoding scheme for quantum simulations of electronic structure. Physical Review Research, 4:023154, May 2022.

[18] Dave Wecker, Bela Bauer, Bryan K. Clark, Matthew B. Hastings, and Matthias Troyer. Gate-count estimates for performing quantum chemistry on small quantum computers. Physical Review A, 90(2), August 2014.

doi:10.6342/NTU202401735

[19] Sergey Bravyi, Jay M. Gambetta, Antonio Mezzacapo, and Kristan Temme. Tapering off qubits to simulate fermionic Hamiltonians, 2017.

[20] Andrew Tranter, Peter J. Love, Florian Mintert, and Peter V. Coveney. A comparison of the Bravyi–Kitaev and Jordan–Wigner transformations for the quantum simulation of quantum chemistry. Journal of Chemical Theory and Computation, 14(11):5617–5630, September 2018.

[21] Jonathan Romero, Ryan Babbush, Jarrod R. McClean, Cornelius Hempel, Peter Love, and Alán Aspuru-Guzik. Strategies for quantum computing molecular energies using the unitary coupled cluster ansatz, 2018.

[22] Abhinav Kandala, Antonio Mezzacapo, Kristan Temme, Maika Takita, Markus Brink, Jerry M. Chow, and Jay M. Gambetta. Hardware-efficient variational quantum eigensolver for small molecules and quantum magnets. Nature, 549(7671):242–246, September 2017.

[23] Jarrod R. McClean, Sergio Boixo, Vadim N. Smelyanskiy, Ryan Babbush, and Hartmut Neven. Barren plateaus in quantum neural network training landscapes. Nature Communications, 9(1), November 2018.

[24] Shih-Kai Chou, Jyh-Pin Chou, Alice Hu, Yuan-Chung Cheng, and Hsi-Sheng Goan. Accurate harmonic vibrational frequencies for diatomic molecules via quantum computing. Physical Review Research, 5:043216, Dec 2023.

doi:10.6342/NTU202401735